Mapping Phosphate Modifications of Substituted Lipid A via a Targeted MS^3 CID/UVPD Strategy

Christopher M. Crittenden[†], *Carmen M. Herrera*[‡], *Peggy E. Williams*[†], *Dante P. Ricci*[§], *Lee R. Swem*[§], *M. Stephen Trent*[‡], *Jennifer S. Brodbelt*[*,†]

[†] Department of Chemistry, University of Texas at Austin, Austin, Texas 78712, USA
[‡] Department of Infectious Diseases, University of Georgia, Athens, Georgia 30602, USA
[§] Achaogen, Inc., 1 Tower Place, South San Francisco, CA, 94080, USA

[*] Phone: (512) 471-0028, E-mail: brodbelt@cm.utexas.edu

Supplemental Information

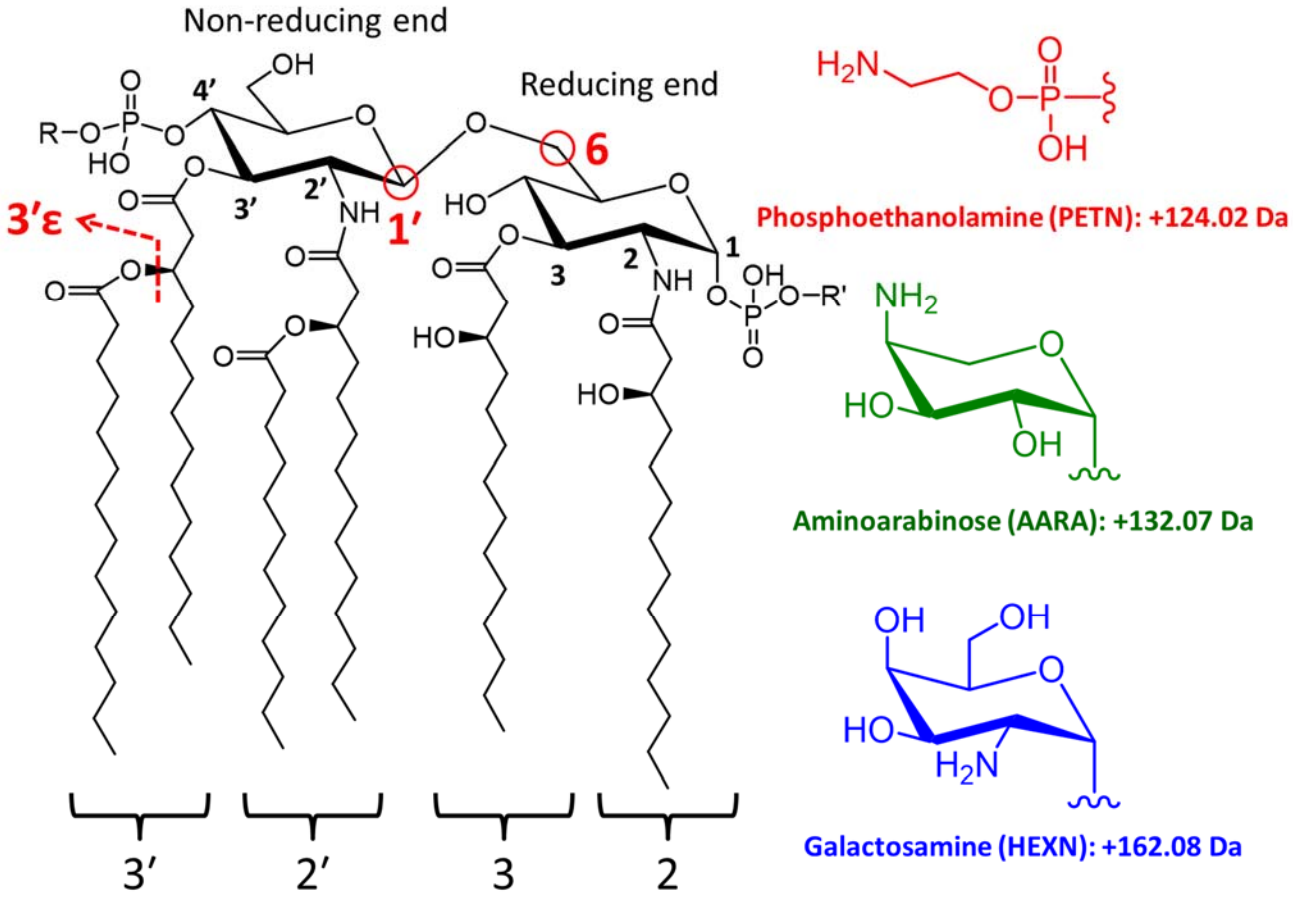

Figure S1: Structure of a typical hexaacylated lipid A. Potential substitutions are shown at the right: phosphoethanolamine (PETN, red); aminoarabinose (AARA, green); galactosamine (HEXN, blue).

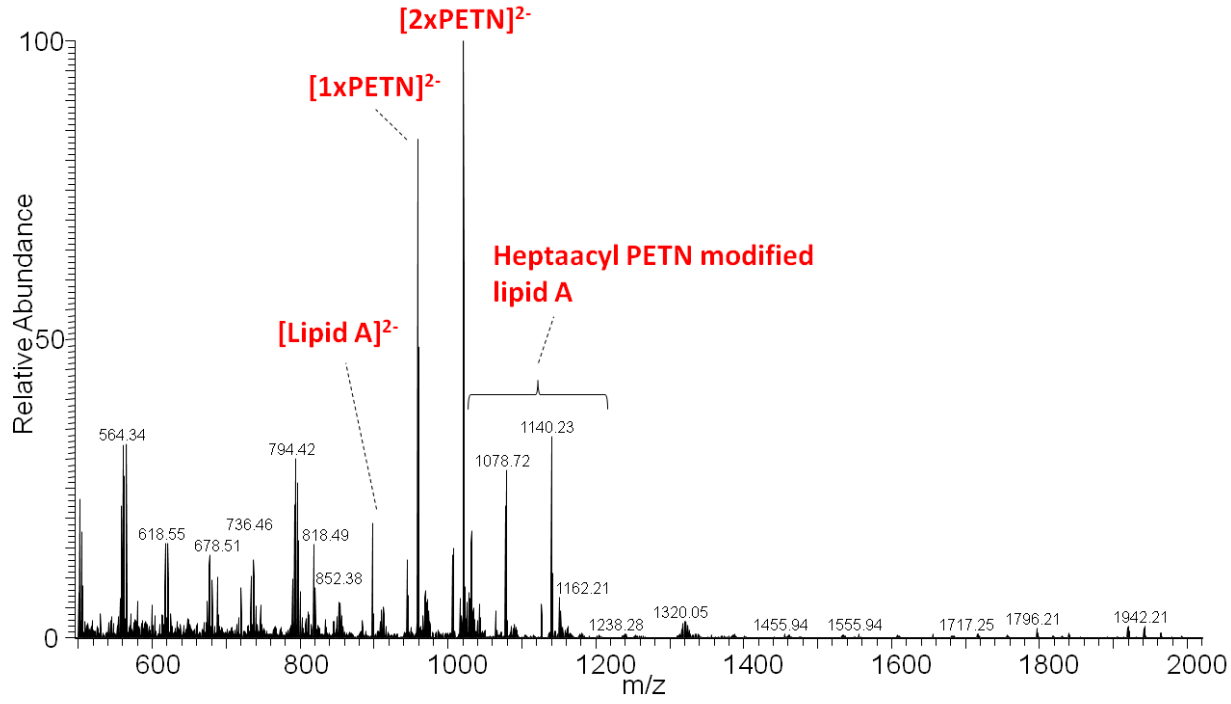

Figure S2. MS[1] spectrum of the sample SLAM 1. The region from *m/z* 500 to 850 is typically congested with other biological contaminants and detergents utilized in the sample preparation procedure.

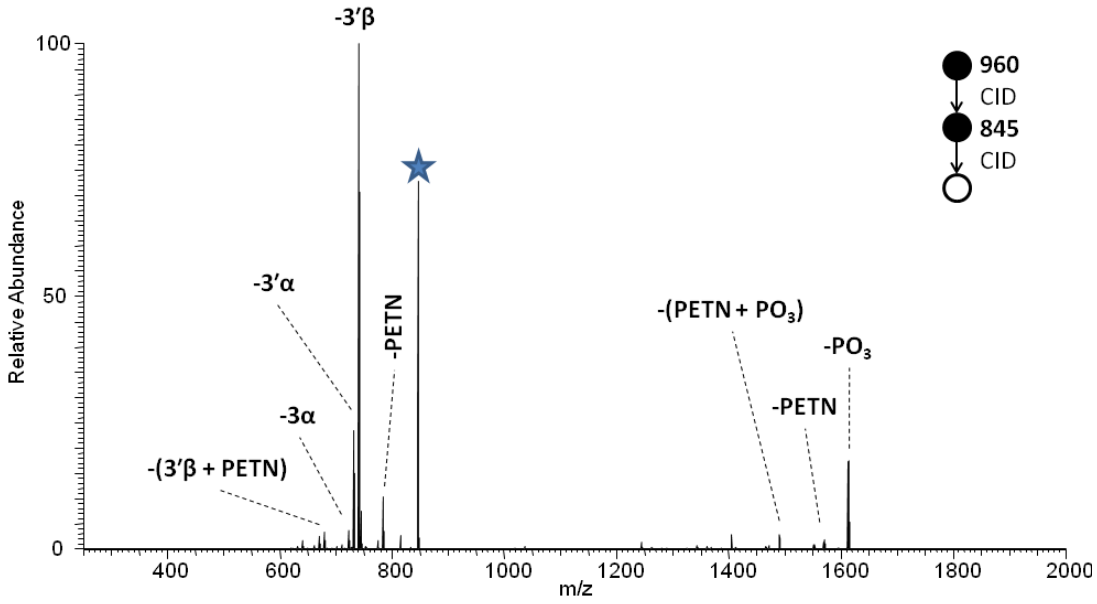

Figure S3: CID/CID (MS^3) of the product ion corresponding to the loss of the 3′ε acyl chain (*m/z* 845, 2-)) from the singly PETN-modified lipid A (m/z 960, 2-) from SLAM 1 in **Figure 2a**. Localization of the PETN moiety is not achieved through this method as the diagnostic fragments from glycosidic cleavages are absent. Note that the MS^2 spectrum is shown in **Figure 3a**.

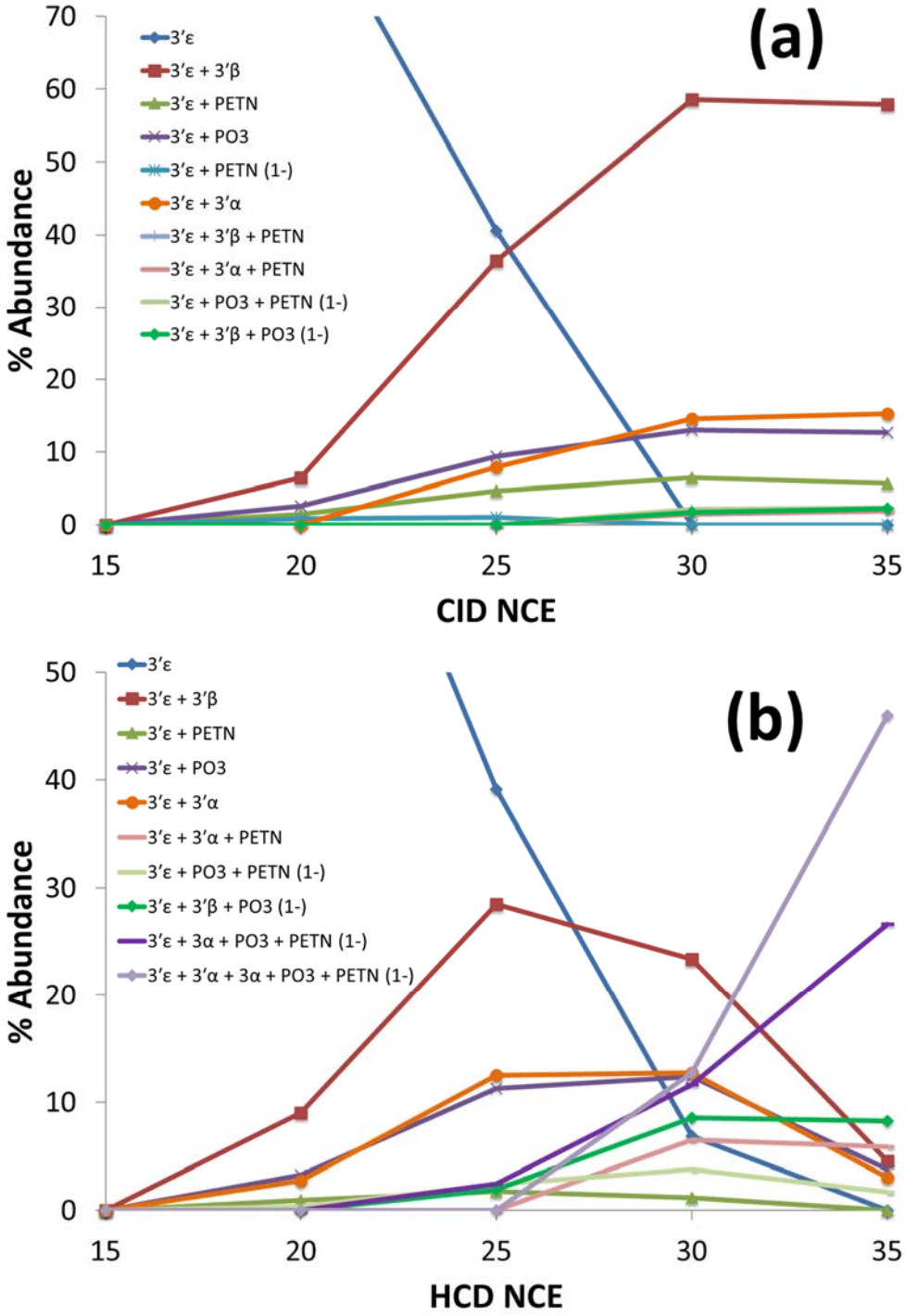

Figure S4: Energy variable CID/CID (a) and CID/HCD (b) of the product ion corresponding to the loss of 3′ε acyl chain (*m/z* 845, 2-) of the singly PETN-modified lipid A from SLAM 1 in **Figure 2a**. The CID spectrum of the singly PETN-modified lipid A from SLAM 1 is shown in **Figure 3a**, and the loss of the 3′ε acyl chain is highlighted in green. Combinatorial losses of primary acyl chains, PETN, and PO_3 are the most dominant ions produced in this experiment.

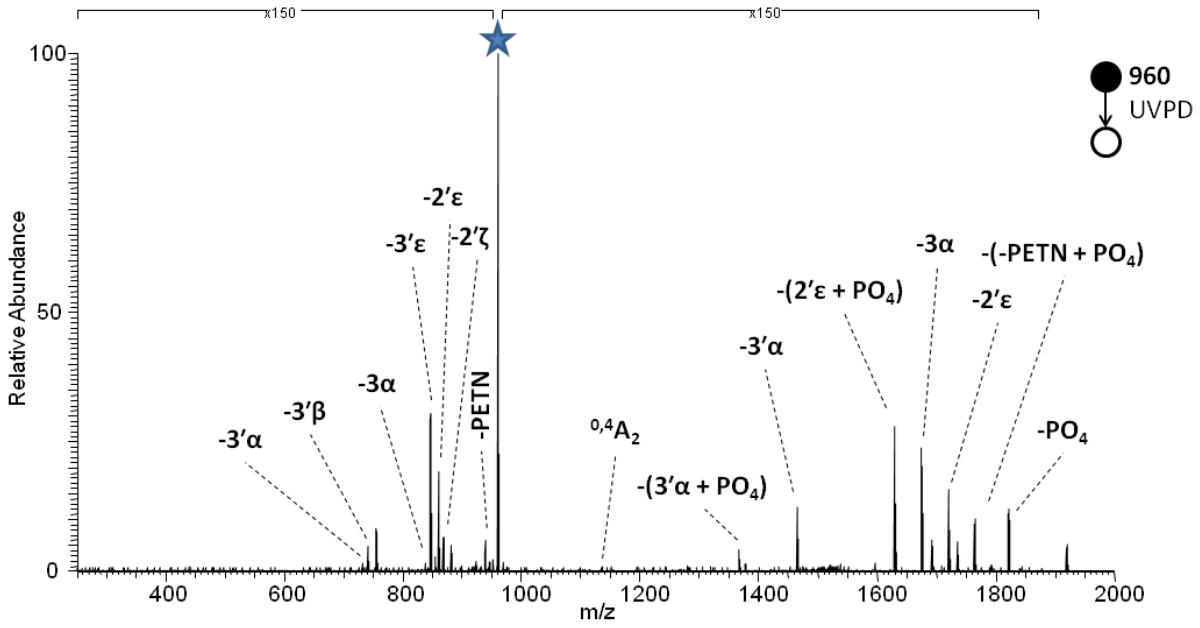

Figure S5: UVPD (MS^2) of the PETN-modified lipid A (*m/z* 960, 2-) from SLAM 1 in **Figure 1a**. UVPD allows localization of the PETN moiety via detection of the $^{0,4}A_2$ cross-ring cleavage product but with lower abundance than the CID/UVPD method (**Figure 3**).

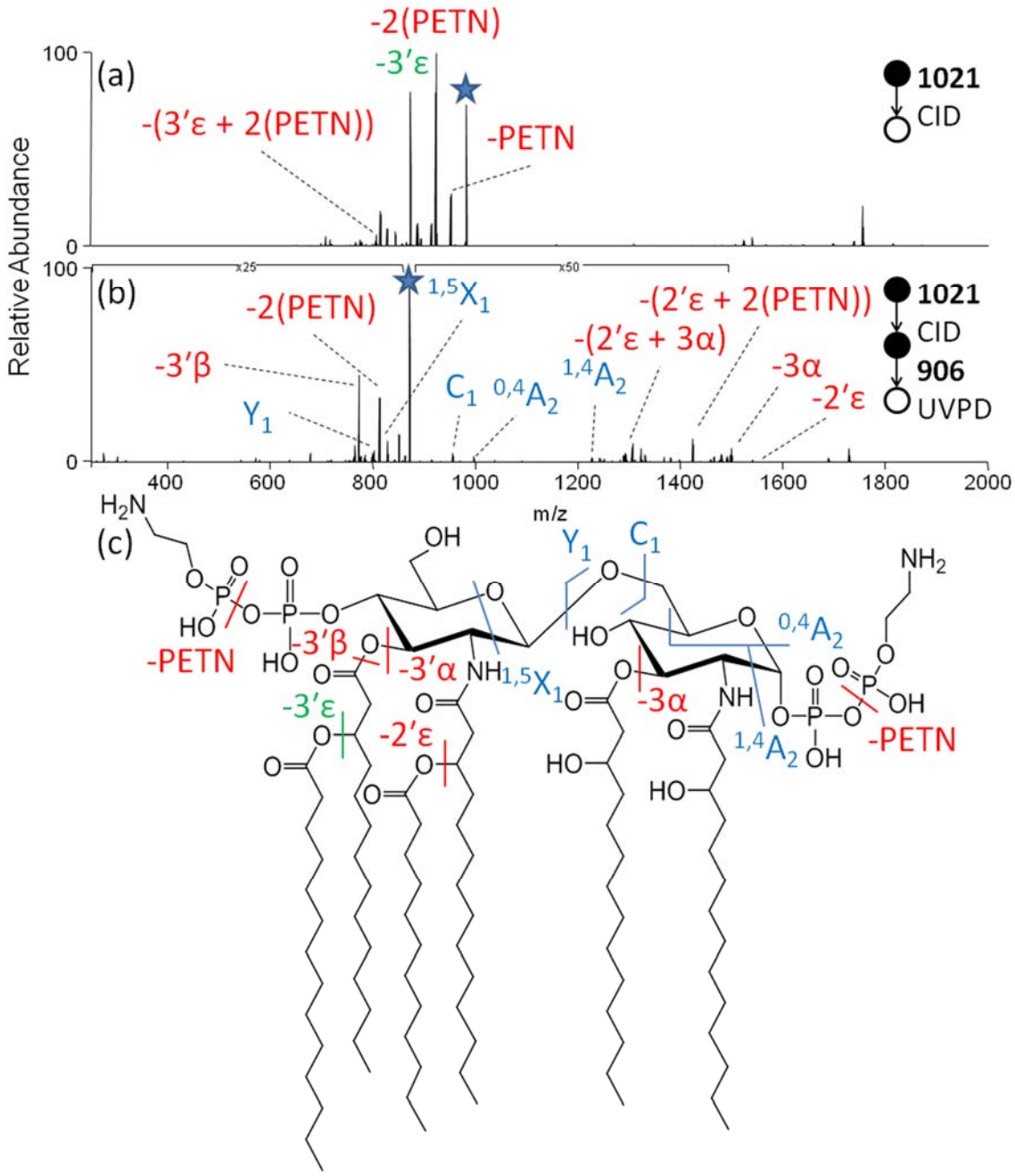

Figure S6: (a) CID of bis-PETN substituted lipid A of *m/z* 1021 (2-) from SLAM 1 reveals labile acyl chain losses as well as a diagnostic neutral loss associated with PETN modifications. (b) UVPD of the ion corresponding to the loss of the 3′ε acyl chain (*m/z* 906, 2-) provides diagnostic product ions that allow localization of the PETN substitution to the 4- and 1′-phosphate positions, as shown in (c), while additional identifications are shown in red.

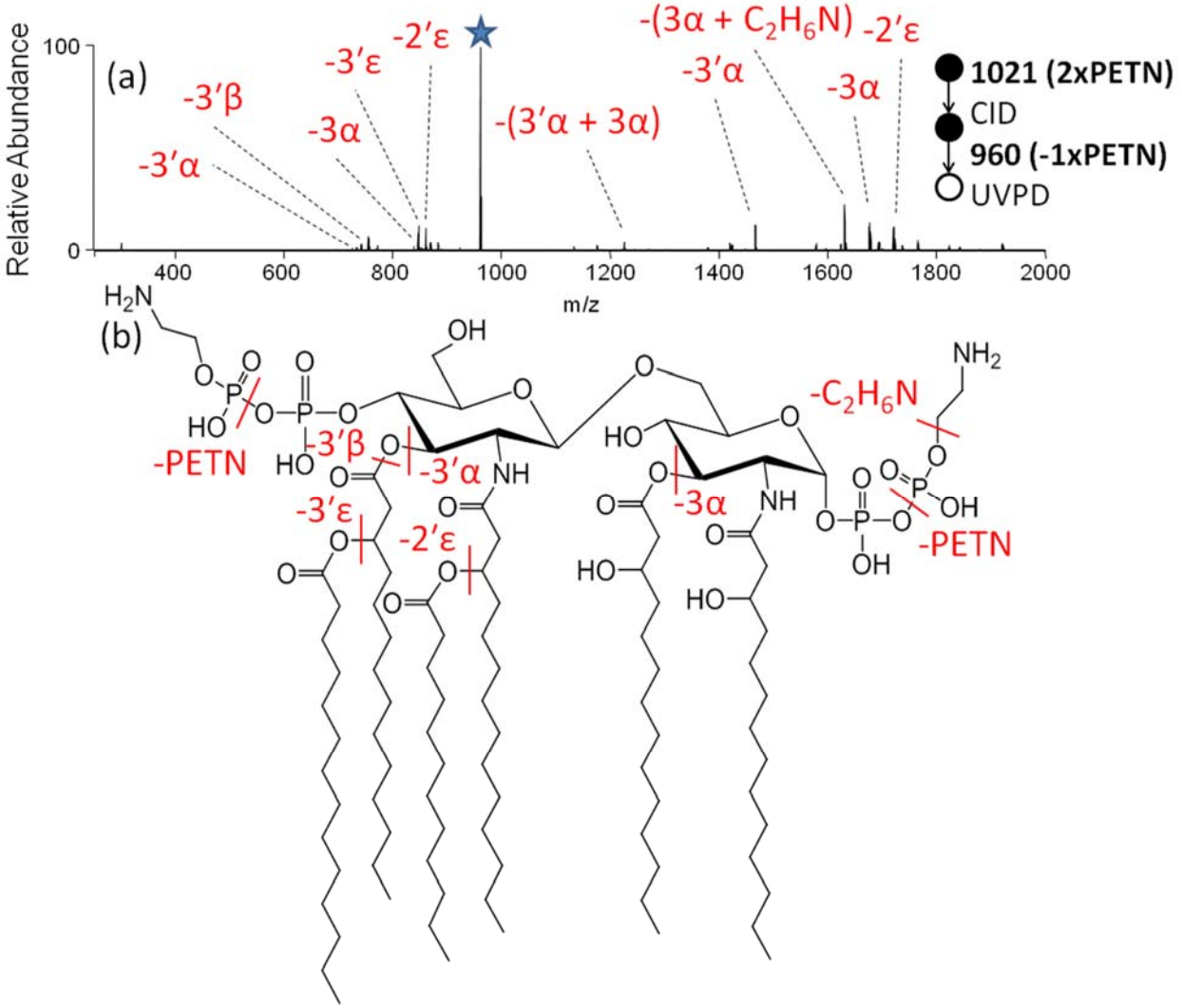

Figure S7: (a) UVPD of bis-PETN substituted lipid A of the ion corresponding to the loss of a single PETN moiety (*m/z* 960, 2-) as produced by CID of the precursor ion of *m/z* 1021 (2-). A combination of acyl chains were indentified from this workflow (b), however diagnostic glycosidic fragmentation is absent.

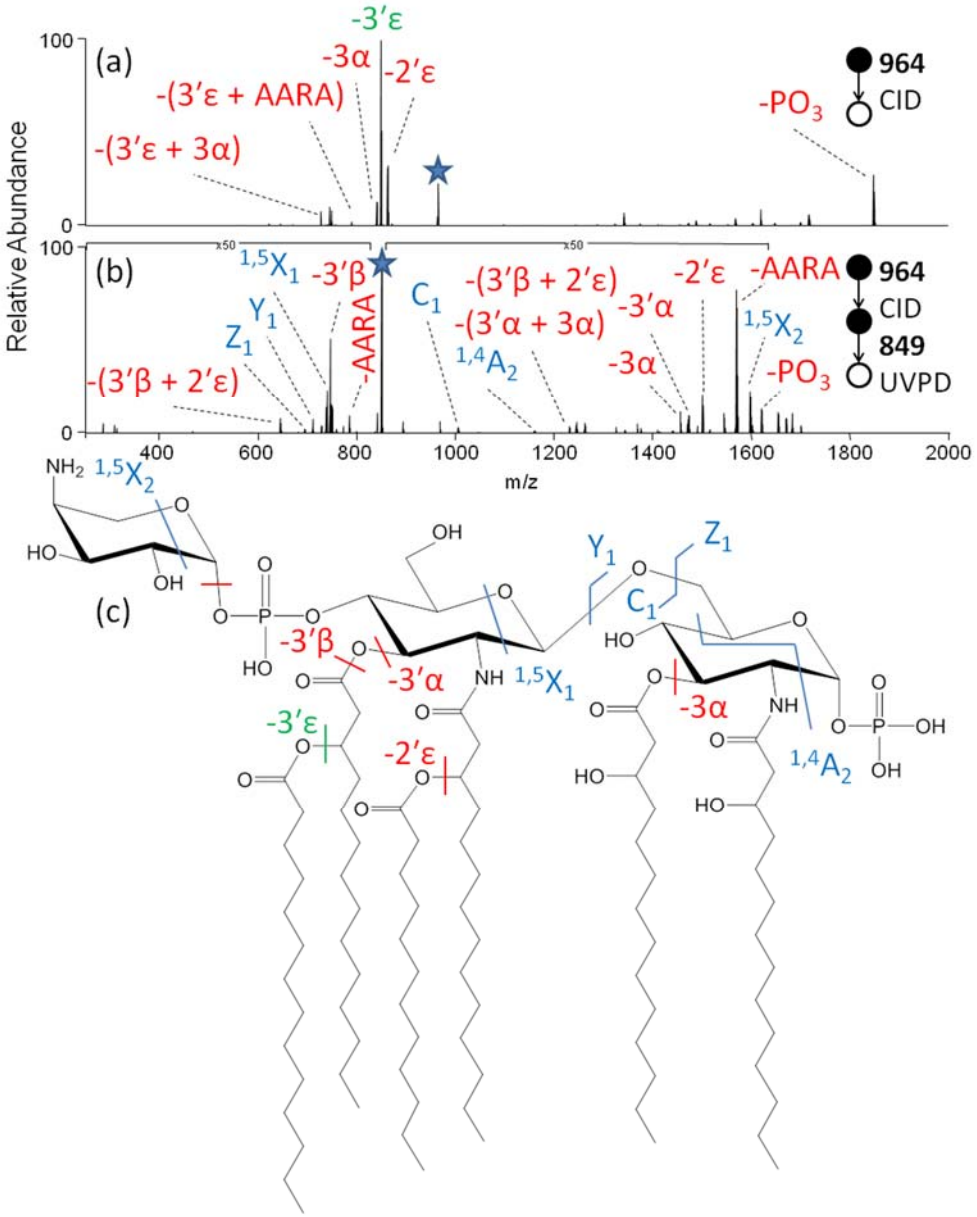

Figure S8: (a) CID of substituted lipid A from SLAM 2 at *m/z* 964 (2-) reveals labile acyl chain losses as well as a diagnostic neutral loss associated with AARA modifications. (b) UVPD of the ion corresponding to the loss of the 3′ε acyl chain (*m/z* 849, 2-, labeled green) provides diagnostic product ions (shown in blue) that allow localization of the AARA substitution to the 4′-phosphate position, as shown in (c), while additional identifications are shown in red. The selected precursor ion in each stage is marked with a star.

Table S1: Diagnostic fragment ions for 1xPETN lipid A from SLAM 1 (**Figure 3**). The *m/z* value of the precursor is given along the *m/z* value of the ion corresponding to the loss of the 3′ε acyl chain, and the *m/z* values for the diagnostic glycosidic fragment ions identified.

Fragment Ion ID	MS^n	Theoretical (*m/z*)	Observed (*m/z*)	ppm error
[M-2H] (1xPETN)	MS^1	959.610	959.609	-1.042
3′ε	MS^2	845.002	845.003	1.183
$^{1,4}A_2$	MS^3	1148.569	1148.566	-2.612
$^{0,4}A_2$	MS^3	914.576	914.553	-25.148
$^{1,5}X_1$	MS^3	861.428	861.431	3.483
Y_1	MS^3	833.433	833.439	7.120
Z_1	MS^3	818.446	818.449	3.665

Table S2: Diagnostic fragment ions for 2xPETN lipid A from SLAM 1 (**Figure S6**). The *m/z* value of the precursor is given along with the *m/z* value of the ion corresponding to the loss of the 3′ε acyl chain, and the *m/z* values for the diagnostic glycosidic fragment ions.

Fragment Ion ID	MS^n	Theoretical (*m/z*)	Observed (*m/z*)	ppm error
[M-2H] (2xPETN)	MS^1	1021.115	1021.113	-1.959
3′ε	MS^2	906.507	906.506	-1.103
$^{1,4}A_2$	MS^3	1274.601	1274.585	-12.553
$^{0,4}A_2$	MS^3	1040.608	1040.611	2.883
C_1	MS^3	996.582	996.589	7.024
$^{1,5}X_1$	MS^3	861.428	861.428	0.000
Y_1	MS^3	833.433	833.435	2.400

Table S3: Diagnostic fragment ions for 1xAARA lipid A from SLAM 2 (**Figure S8**). The *m/z* value of the precursor is given along with the *m/z* value for the ion corresponding to the loss of the 3′ε acyl chain, and the *m/z* values for the diagnostic glycosidic fragment ions.

Fragment Ion ID	MS^n	Theoretical (*m/z*)	Observed (*m/z*)	ppm error
[M-2H] (1xAARA)	MS^1	963.635	963.632	-3.113
3′ε	MS^2	849.027	849.027	0.000
$^{1,5}X_2$	MS^3	1595.998	1595.999	0.627
$^{1,4}A_2$	MS^3	1156.620	1156.619	-0.865
C_1	MS^3	1003.624	1003.623	-0.996
$^{1,5}X_1$	MS^3	738.419	738.420	1.354
Y_1	MS^3	710.424	710.425	1.407

Table S4: Diagnostic fragment ions for 1xPETN 1xHEXN lipid A from SLAM 3 (**Figure 4**). The *m/z* value of the precursor is given along with the *m/z* value of the ion corresponding to the loss of the 3′ε acyl chain, and the *m/z* values for the diagnostic glycosidic fragment ions identified.

Fragment Ion ID	MS^n	Theoretical (*m/z*)	Observed (*m/z*)	ppm error
[M-2H] (1xPETN 1xHEXN)	MS^1	1098.187	1098.165	-20.033
3′ε	MS^2	997.090	997.086	-4.012
$^{0,4}A_2$	MS^3	1029.579	1029.569	-9.713
$^{1,5}X_1$	MS^3	1054.632	1054.641	8.534

Table S5: Diagnostic fragment ions for 2xAARA lipid A from SLAM 4 100 PMB (**Figure 5**). The *m/z* value of the precursor is given along with the *m/z* value of the ion corresponding to the loss of the 3′ε acyl chain, and the *m/z* values for the diagnostic glycosidic fragment ions identified.

Fragment Ion ID	MS^n	Theoretical (*m/z*)	Observed (*m/z*)	ppm error
[M-2H] (2xAARA)	MS^1	1044.188	1044.183	-4.788
3′ε	MS^2	929.076	929.074	-2.152
$^{0,4}A_2$	MS^3	1075.682	1075.684	1.859
C_1	MS^3	1031.655	1031.658	2.908
$^{1,5}X_1$	MS^3	869.478	869.480	2.300
Y_1	MS^3	841.483	841.485	2.377